Catalysis Today 161 (2011) 29–34

Contents lists available at ScienceDirect

Catalysis Today

journal homepage: www.elsevier.com/locate/cattod

Photocatalytic properties of different TiO_2 thin films of various porosity and titania loading

Jiří Zita[a,*], Josef Krýsa[a], Urh Černigoj[b], Urška Lavrenčič-Štangar[b], Jaromír Jirkovský[c], Jiří Rathouský[c]

[a] Institute of Chemical Technology Prague, Department of Inorganic Technology, Technická 5, CZ-166 28 Prague, Czech Republic
[b] Laboratory for Environmental Research, University of Nova Gorica, Vipavska 13, P.O. Box 301, 5001-SI Nova Gorica, Slovenia
[c] J. Heyrovskyĭ Institute of Physical Chemistry of the ASCR, v.v.i., Dolejškova 3, 18223 Praque, Czech Republic

ARTICLE INFO

Article history:
Received 30 June 2010
Received in revised form
23 November 2010
Accepted 25 November 2010
Available online 22 January 2011

Keywords:
Sol–gel
Titanium dioxide film
Porosity
Photocatalysis
Degradation of dyes in an aqueous solution
Degradation of thin layers

ABSTRACT

Thin sol–gel titania films with varying porosity but constant mass were coated on SiO_2/glass substrate. The mass was kept constant by changing the withdrawal rate of dipping from a titania sol. The porosity properties of the films were determined by the analysis of adsorption isotherms of Kr at ca 77 K.

Photocatalytic performance of TiO_2 layers in the degradation of Acid orange 7 (AO7) and 4-chlorophenol (4CP) in aqueous solution depends on the mass of titania but not on the porosity/surface area of the films. On the contrary, in the degradation of thin layers of Resazurin (Rz) ink and methyl stearate (MS) deposited on the TiO_2 film surface, the activity of the films is clearly enhanced due to the porosity but does not depend on titania mass itself.

Obtained data suggest that while in an aqueous solution the reaction rate depends primarily on the mass of titania and amount of absorbed light, in solid thin films test the porosity/surface area together with interfacial area of tested compound with titania layer is significant.

1. Introduction

Thin films of titanium dioxide deposited on various supports are very useful photocatalysts in a number of applications. In aqueous media, the rather demanding and time-consuming separation of the photocatalytic material is avoided, as the films are firmly fixed to their supports. Further the coating of the surface of a number of products as well as the external surfaces of buildings and other constructions enables to render them self-cleaning or at least easy-to-clean [1]. Such a distinguished property would substantially enhance the utility value of the products and would improve the cleanness of the environment and consequently the quality of life. The photocatalytically active coatings can oxidatively decompose organic deposits to inorganic products, such as CO_2, H_2O and mineral acids [2,3]. Consequently, the dust particles will no more stick on the irradiated surface and can be easily washed off by rain water. Additionally, such finishes often exhibit photoinduced superhydrophilicity, which further improves their self-cleaning ability.

However, there are two important aspects which should be addressed. As the films are often thin, mostly only several tens or hundreds of nanometres in thickness, the amount of photocatalytically active material is generally small. Consequently, the light absorption is often limited, which may negatively affect the photocatalytic performance. Second the films may be either compact or porous, which provides an interesting tool how to control their performance. The porous films of TiO_2 may be more effective when the photodecomposition mechanism includes reactants or intermediates adsorbed on the surface. Further the mesoporosity may ensure fast transport of O_2 and H_2O, which are viable for the photocatalytic degradation of deposited layers of dirt and can be significantly hindered due to the compactness of those layers [4,5].

Due to large variability of potential applications (self-cleaning surfaces, water and air purification, etc.) we have decided to use different model compounds for a photocatalytic activity tests. We used ionic organic dye (Acid orange 7) and neutral organic molecule (4-chlorophenol) in water solutions, fatty acid ester (methyl stearate) and reductively degraded substance (Resazurin ink) in thin film.

Glass support enabled the characterization of the layers by UV/vis absorption spectroscopy. SiO_2 interlayer prevented diffusion of sodium ions from glass to TiO_2 photocatalytic layer [6]. Sol–gel combined with surfactant addition was used to synthesize well defined porosity of titana layers.

Clearly, the combined effect of the variation in the light absorption and the films' porosity on their photocatalytic performance markedly depends on the system tested. Therefore the present

* Corresponding author. Tel.: +420 220 444 112; fax: +420 220 444 410.
E-mail address: Jiri.Zita@vscht.cz (J. Zita).

0920-5861/$ – see front matter © 2010 Elsevier B.V. All rights reserved.
doi:10.1016/j.cattod.2010.11.084

study is aimed at the analysis of the films' porosity and their light absorption and the correlation of these properties with the photocatalytic performance in several important systems, namely the degradation of selected dyes dissolved in water and the decomposition of thin layers of model dirt.

2. Experimental

2.1. Chemicals

Absolute ethanol, 36% hydrochloric acid, 65% nitric acid were purchased from Penta, sodium acetate and ethyl acetoacetate (EAA) from Riedel-de Haen, 2-methoxyethanol from Fluka, Pluronic F-127, polyoxyethylene(10)cetyl ether (Brij 56). 97% Titanium(IV) isopropoxide ($Ti(OiPr)_4$) (Sigma–Aldrich) and 98% tetraethyl orthosilicate TEOS (Fluka) were used for the preparation of TiO_2/SiO_2/glass films. Glycerol (99.5% Sigma–Aldrich) and hydroxyethyl-cellulose (Fluka) were used for the preparation of the Rz ink. The dyes Acid orange 7 (AO7) (dye content ~85%), and ResazurinRz (dye content ~92%) and 4-chlorophenol 4-CP (≥99%) were supplied by Sigma–Aldrich, methyl stearate (MS) by Fluka and n-hexane by Carlo Erba. All the chemicals were used as received.

2.2. Preparation of TiO_2/SiO_2/glass samples

First a SiO_2 barrier layer ca 50 nm in thickness was deposited on the microscope soda-lime glass slides (75 × 25 1 mm) as follows: 10 g of TEOS was diluted with 15 mL of ethanol and stirred for 90 min. Afterwards 2.5 mL of water and 0.5 mL of concentrated hydrochloric acid were added to produce a sol, which was stirred for 1 h. The sol could be stored for up to 1 month in cold and dark. The microscope slides were dip-coated (at a withdrawal rate of 60 mm min^{-1}) with the SiO_2 sol and was calcined at 550 °C for 3 h to obtain a SiO_2 barrier layer.

Transparent TiO_2 films were deposited on both sides of SiO_2-precoated glass slides by a sol–gel route, already described in detail in our previous publications [7,8]. $Ti(OiPr)_4$ was added to EAA (n(EAA)/n(Ti(OiPr)4) = 1) at constant stirring. The prepared solution was dissolved in 2-methoxyethanol ($n(MeOCH_2CH_2OH)/n(Ti) = 13.6$) and was stirred at room temperature at least for 3 h (sol D). The prepared sol was kept in the refrigerator and was conditioned at room temperature for at least 1 h before the use. The procedure for the preparation of modified sols with added surfactants or copolymers was basically the same as described above. The only difference was that the triblock copolymer Pluronic F-127 (4.7 g) or surfactant Brij 56 (15 wt.%) were dissolved in the sol (35.0 g) after the addition of 2-methoxyethanol to form sol C and sol R, respectively. Sol L was prepared at vigorous stirring, 7 g of $Ti(OiPr)_4$ solution being added drop wise to 10 ml of ethanol. Afterwards, 10 ml of ethanol, 2 g of ethyl acetoacetate and nitric acid were then added and the mixture was stirred for 24 h. The obtained sol could be stored for up to 3 months in dark and cold [9].

To keep the mass of titania in TiO_2 layers prepared from sols C, D, R and L constant, different withdrawal rates of the dip-coating were used. The deposited films were calcined at 500 °C for 1 h.

2.3. Titania layer characterisation

The adsorption experiments were carried out using an Micromeritics ASAP 2010 apparatus. Prior to the adsorption experiments the samples were outgassed at 200 °C overnight. In order to determine the texture parameters of thin porous films deposited on supports, whose total surface area is in the range of several tens of square centimeters, a high-sensitive Kr adsorption technique has to be used. The most frequently used adsorptives, namely, nitrogen and argon at ca 77 and 87 K, respectively, cannot be applied with materials having very small surface area. The saturation pressures of nitrogen and argon at 77 and 87 K, respectively, are very high, reaching ca 760 Torr, which leads to an extremely large number of molecules being trapped within the void volume of the sample cell. Because of the very small total pore volumes and surface areas of such thin porous films, the pressure changes due to adsorption cannot be measured with sufficient precision. As an alternative, an adsorptive with a substantially lower saturation vapor pressure should be used, such as krypton at the boiling point of liquid nitrogen, whose saturation pressure equals 1.63 Torr and 2.63 Torr as a solid and a supercooled liquid, respectively.

The specific surface area was determined by the BET method using the molecular cross-sectional area of Kr of 0.21 nm^2 as suggested by the producer of the equipment. The information on the pore volume was obtained from the limiting adsorption at pressure near to the saturation pressure. As the analysis of adsorption isotherms of Kr at 77 K is far from being straightforward and a well-established procedure (e.g. DFT) has not been implemented yet, a simple method based on comparative plots was used to determine the mean pore size and the pore size distribution [5]. First, a non-porous anatase (Aldrich) was selected as a suitable reference material, whose surface area equalled 11.2 $m^2\,g^{-1}$. On this material, the adsorption isotherm of Kr at 77 K was carefully measured several times with a very good reproducibility. This isotherm was afterwards used as a reference in the calculation of the pore size distribution. Second, comparative plots for each sample were constructed, in which the adsorption on the sample under study was plotted against that on the reference material. If such a plot provided a straight line, the mechanism on both the non-porous reference material and the sample under study should be the same, i.e. also the sample under study would be non-porous, the slope of the straight line giving its surface area. Any upward deviation from the linearity indicates the presence of porosity, which was actually the case for all the samples studied. The degree of this deviation and location correspond to the amount and size of the pores. Third, the comparative plots were differentiated, which provided an assessment of the pore size distribution for each film.

Finally, the x-axis of the differentiated comparison plot was converted from the adsorption on the reference material to the pore width. To obtain an equation enabling such a conversion, adsorption isotherms of Kr at 77 K were measured on a series of powders of mesoporous TiO_2 with structure and texture properties as similar as possible to the samples studied. The texture properties of these powders were reliably determined from the analysis of adsorption isotherms of nitrogen at 77 K using a DFT method.

The mass of TiO_2 layer was determined by measuring the weight of glass with and without titania layer using balance. The coated area varied depending on used titania sol and was $9.5 \pm 0.5\ cm^2$. The thickness of the films was measured by a Taylor–Hobson Talysurf profilometer. The crystallinity of the films was determined with an X'Pert PRO θ–θ powder diffractometer with a parafocusing Bragg–Brentano geometry using Cu K_α radiation.

The transmittance (T) and reflectance (R) spectra (300–700 nm spectral range) of clean and calcined TiO_2 films deposited on SiO_2-precoated sodium glass were recorded on UV–vis–NIR spectrophotometer Lambda 950 (PerkinElmer) employing an integration sphere with inner diameter of 150 mm (PELA 1000, PerkinElmer). When measuring T spectra, the sample was inclined 11° from the normal direction of an incoming radiation beam of the spectrometer to get the optical interference maxima and minima at exactly the same wavelength values as in reflectance spectra. According to Eq. (1), the sum of T and R spectra was subtracted from

1 in order to obtain the true absorption (A) of the investigated TiO_2 film:

$$T + R + A = 1 \quad (1)$$

The adsorption (A) for the wavelength of 365 nm was calculated for all prepared films and compared with other layer properties like mass and thickness.

2.4. Photocatalytic experiments

2.4.1. AO7 and 4CP degradation

Stirred, air saturated aqueous solutions of model compounds AO7 (10^{-5} M, pH = 6.6, 25 cm^3) and 4-CP (10^{-4} M, pH = 4.5, 25 cm^3) were photocatalytically oxidized on TiO_2 films in a glass cuvette (2.0 cm path length × 3.0 cm × 5.0 cm depth) at 20 °C (no air or O_2 bubbling was provided). The irradiation was provided by UVA light (1.5 mW cm^{-2}) from an 11 W BLB Sylvania Lynx light source (wavelength range from 320 to 390 nm with maximum at 355 nm). The concentration of 4-CP and AO7 was determined by HPLC (Shimadzu 10avp) and UV–vis spectrophotometry (Varian 100), respectively.

In the test, the solution was first equilibrated with the titania film for 45 min in the dark to ensure a complete adsorption of the test compound. A simple spectroscopic analysis of the AO7 solution before and after this equilibration step revealed that in all cases less than 2% of the compound tested was adsorbed by the titania films. In the case of 4-CP, the adsorption was even lower (within the error of measurement).

2.4.2. Rz ink

The Rz ink used in this work comprised 3 g of 1.5% aqueous solution of hydroxycellulose (HEC), 0.3 g of glycerol and 4 mg of the redox dye, Resazurin, Rz [10]. A film of the ink was coated (withdrawal speed 60 mm min^{-2}) onto the substrate under test and dried in an oven at 70 °C for 10 min. A typical dried ink film was ca 500 nm thick and blue in colour. In this work, each Rz ink coated TiO_2/SiO_2/glass film was irradiated using the same light source as that used in the contact angle test.

In the first step of Rz ink degradation, the blue Rz is reduced by photogenerated electrons to pink resorufin (Rf). Rf can be reduced subsequently to its colourless counterpart dihydroresorufin (HRf) [10]. The degradation rate of Rz ink was then calculated from the first reduction step of the reaction and that is the reason why we are talking about reduction of Rz ink.

2.4.3. Contact angle – MS

The titania films were pre-irradiated in a photochamber (type of the lamps: CLEO 20 W, 438 mm × 26 mm, Philips; broad maximum at 355 nm) for 24 h. The photon flow (Φ_p) in the cell was evaluated by potassium ferrioxalate actinometry [11], and determined to be 5.3×10^{-9} Einstein cm^{-2} s^{-1}. The methyl stearate coatings were prepared from a solution of methyl stearate in n-hexane (0.2 M) by dip-coating at a withdrawing speed of 20 cm min^{-1}. After the pre-irradiation, the methyl stearate was deposited. Then the films were positioned back in the photochamber on places with the same UVA intensities and were irradiated for a certain time in air at 25 °C. The degradation of methyl stearate was followed by measuring the water CA at room temperature using a horizontal microscope with a protractor eyepiece. To this aim, a Contact Angle Meter (CAM-100), KSV Instrument, Ltd., Finland, was used. Specimens were taken out of the illumination chamber for CA measurements after irradiation for different times. The data reported herein correspond to the stable value of the angles obtained by averaging three repeated measurements.

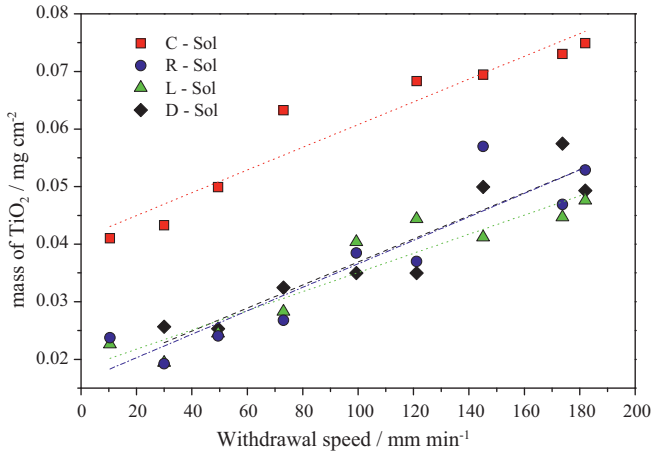

Fig. 1. Amount of TiO_2 [mg cm^{-2}] laid on SiO_2/glass substrate as a function of withdrawal speed [mm min^{-2}] for different titania sols.

3. Results and discussion

One of the goals was to prepare TiO_2 layers on SiO_2/glass substrate from four different sols (sols C and R for mesoporous and sols L and D for titania layers of low porosity). For a better comparison of titania layers with different morphological properties it is very useful to keep one parameter constant, the mass of TiO_2 being chosen. Fig. 1 shows the amount of TiO_2 [mg cm^{-2}] deposited on SiO_2/glass substrate as a function of withdrawal speed [mm min^{-1}] for different titania sols. It is obvious that the preparation of layers with the same amount of titania from sols D, L and R is easy. With the sol C, layers prepared at very low withdrawal speeds (<60 mm min^{-1}) were not transparent (milky mist appeared after calcinations). For higher withdrawal speeds (≥60 mm min^{-1}) the mist disappeared, but the amount of titania in such layers was the same as the maximal amount which can be reached using sols D, L and R.

Two different withdrawal rates were used for each titania sol to create TiO_2 layers with different mass of titania. The withdrawal rates together with the mass of prepared titania films are in Table 1. The samples 1 (C1, R1, L1 and D1) have almost the same mass of titania.

3.1. Titania layer characterization

3.1.1. Porosity

According to their texture properties, the samples can be divided into three groups.

Films C1 are characterized by well-developed mesoporosity with large surface area and pore volume (Table 1, Fig. 2). Especially the sample C1 exhibits an unusually high porosity of 64%. As both the adsorption and desorption branches of the isotherm on C1 is very steep (Fig. 2), this sample have a narrow pore size distribution. The average pore size of C1 is roughly 10–11 nm. The analysis using the above described semiempirical method shows that the pores are definitely larger than 10 nm. More specific statement is difficult, as this method is not suitable for so wide pores.

The isotherm on sample R1 is substantially flatter than that on C1, which indicates a rather broad pore size distribution. The porous system of the sample R1 seems different from that of C1. First, pores of R1 are definitely narrower; second also some proportion of smaller mesopores is contained. Therefore this sample has a very high specific surface area.

The D1 and especially L1 films have much less developed porous system, their porosity achieving only 9 and 4% (Table 1). Both isotherms are rather flat with very wide hysteresis loops, reach-

Table 1
An overview of samples, their texture parameters.

TiO_2/SiO_2/ Glass samples	Withdrawal rate [mm min^{-1}]	TiO_2 mass [mg cm^{-2}]	Thickness [a] [nm]	V_{TOT} [a] [$\times10^3$ cm^3]	S_{BET} [a] [cm^2]	S_{sp} [m^2 cm^{-3}]	V_{pore} [a] [$\times10^3$ cm^3]	Porosity [%]	D [nm]
C1	60	0.0607 ± 0.0024	206 ± (37)	0.721	2983	160	0.461	64	10.2
C2	200	0.0779 ± 0.0022	533 ± (18)	–	–	–	–	–	–
R1	150	0.0516 ± 0.0001	201 ± (12)	0.804	2381	296	0.337	42	6
R2	50	0.0317 ± 0.0017	108 ± (27)	–	–	–	–	–	–
L1	200	0.0505 ± 0.0016	146 ± (23)	0.803	267	33	0.033	4	~5
L2	50	0.0265 ± 0.0003	75 ± (12)	–	–	–	–	–	–
D1	175	0.0487 ± 0.0001	148 ± (13)	0.592	350	59	0.052	9	~5
D2	50	0.0307 ± 0.0013	81 ± (29)	–	–	–	–	–	–

V_{TOT}, the total volume of the film including both the voids and the solid pore walls, S_{BET}, the BET surface area, S_{sp}, the specific surface area of a film calculated by dividing the BET surface area by the total volume of a film V_{TOT}. The porosity was calculated by divining the pore volume V_{pore} by the total volume of a film V_{TOT}. D, an assessment of the pore size calculated as $4V_{pore}/S_{BET}$ (formula for calculation of model cylindrical porediameter).

[a] In the fourth column the numbers in brackets represent measured variability in the layer thickness. V_{TOT} was calculated as product of geometrical area of the film and its thickness. The uncertainties of S_{BET} and V_{pore} were about 1% and 3–5%, respectively.

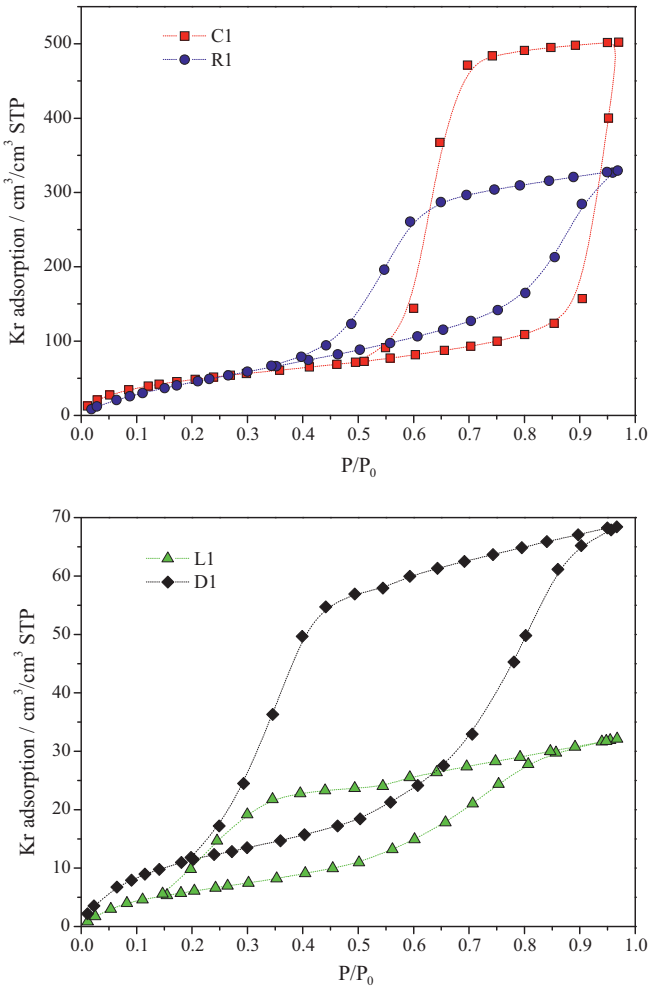

Fig. 2. Adsorption isotherms of Kr at 77 K on the porous films of TiO_2.

ing from relative pressures of 0.1–0.2 to almost 1. Therefore the pore size distribution for both samples is very broad, including also very small mesopores. It is a major difference from samples C1 and C2, which contain only wider pores.

3.1.2. Thickness and mass

Before the measurement of film thickness by profilometry, a part of the titania layer was removed by a mixture of Zn powder with hydrochloric acid, to form the sharp edge. At this edge it was then possible to measure the layer thickness. The results are shown in Table 1 where the numbers in brackets are the differences between profilometry measurements of titania layer thickness on different places of the layer. For all studied films the thickness increases proportionally with mass of titania in the layer. The light absorption depends on the mass of titania, but not on the layer thickness. It means that the optical distance for films with lower and higher porosity is the same.

The thickness of films depends on the withdrawal rate approximately according to the Landau–Levich equation (i.e. thickness is proportional to the rate to the power of 2/3). Similar dependence was found also for their specific surface area and pore volume. The character of porosity (i.e. the pore size, shape and connectivity) is not practically influenced by the withdrawal rate at all [12].

3.1.3. Crystallinity

Typical XRD diffraction patterns of films deposited on SiO_2/glass substrates were observed where the major peak at $2\theta = 25.4$ corresponds to the (1 0 1) reflection of the anatase phase presented in all tested samples (matched with the PDF card 21-1272 [13]). The size of anatase crystallites (calculated by the Scherrer equation) is for films with higher porosity (C, R) 20 nm and for those with lower porosity (L, D) around 12 nm. The only difference between compositions of the films is that C and R sols are modified by the addition of Pluronic F-127 and Brij 56 so it means that the addition of such compounds is increasing not only the porosity but also the anatase crystallite size. On the contrary Dionysiou et al. [14] observed decrease in anatase crystal size when surfactant (Tween 20) was used as modifying agent in sol–gel thin film. The average crystal size of TiO_2 film without surfactant was approximately 11 nm. As the surfactant loading increases, the average crystal size gradually decreases.

3.2. Photocatalytic experiments

3.2.1. Degradation of AO7 and 4CP – aqueous solution

In this work, for each titania film under test a series of UV–vis spectra of the AO7 solution in the spectrophotometric cell were recorded as a function of UVA irradiation time; the results for a typical, L1 layer titania film are illustrated in the insert diagram in Fig. 3. The variation in the absorbance at λ_{max} (485 nm) of the AO7 solution as a function of irradiation time was determined from such data for each of the layered films and the result plotted in the form of AO7 concentration [mol dm^{-3}] vs. irradiation time, illustrated in Fig. 3. From the initial slope of the concentration dependences dc/dt (where the curves are linear: 0–120 min) the initial rate of the dye degradation, R_i [mol min^{-1} cm^{-2}] was then calculated by multiplying the slope by reaction volume and divided by irradiated area of the catalyst layer.

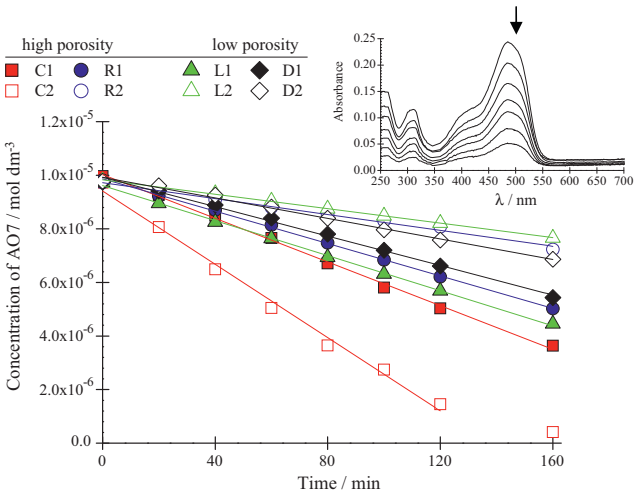

Fig. 3. Diagram of the AO7 concentration (mol dm^{-3}) at 485 nm for different TiO_2/SiO_2/glass films (C1, R1, D1 and L1 having the same mass of titania) as a function of illumination time. The insert diagram is a plot of variation of absorbance spectra of AO7 solution (10^{-5} M) in contact with D1/SiO_2/glass film as a function of UVA (1.5 mW cm^{-2}) irradiation time (one spectrum every 20 min).

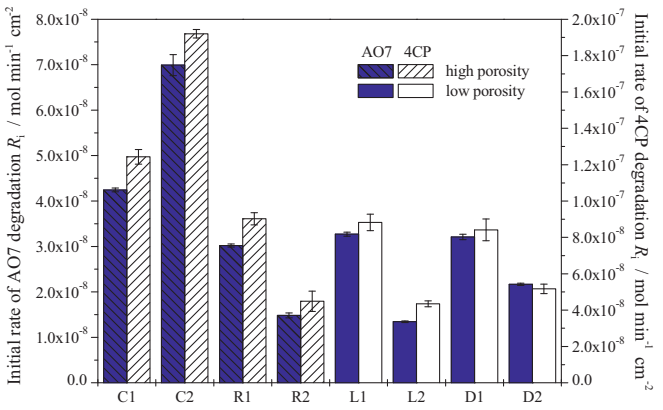

Fig. 4. Initial rates of AO7 and 4CP degradations for TiO_2 films of various porosity and titania loading.

Similarly, each titania film was tested for activity using 4CP as the test compound. 4CP concentration as a function of irradiation time was determined from measured data for each of the layered titania films and again rate of the 4CP degradation, R [mol min^{-1} cm^{-2}] was calculated. The results reveal a rate of 4-CP degradation not too dissimilar to that of AO7.

To see the effect of different porosity and titania loading on AO7 and 4CP degradation, the rates of degradation are shown in Fig. 4. For samples C1, R1, L1 and D1 (same mass of titania but different porosity and surface area) the rate constants are almost the same. If we compare samples with different mass of titana (samples 1 with 2), we can see that the degradation rate depends proportionally on the mass. Please mind that only in layers prepared from sol C, the C2 has higher amount of titania then C1. For all other series (R, L and D) the mass in sample 1 is higher than 2. It is obvious, that the degradation rate of both model compounds depends only on the mass of titania (adsorbed light). The porosity (surface area) is not so important. The results are in good correlation with AO7 degradations on particulate TiO_2 layers (prepared from various titania powders), where the resulting photoactivity does not depend on the surface area of used powders [15].

3.2.2. *Photo-reduction of Rz ink and degradation of MS – solid phase*

All the layered titania films were assessed for photocatalytic activity using the Rz ink test and the spectral variations observed as a function of irradiation time for a typical L1 layer titania film are illustrated in Fig. 5. Note the very short times (every 20 s) between recording each spectrum compared with those for AO7 and 4CP (every 20 min); i.e. the Rz test is more than 60 times faster than the other tests, as well as being simpler to use, under otherwise identical irradiation conditions. The Rz ink reduction was then calculated from the initial linear dependence of Rz adsorption (610 nm) on time.

In order to confirm the results from Rz ink method, its comparison with a standard method (CA measurements during MS degradation) was carried out. Fig. 6 shows the degradation of MS thin film on films with various porosity. For films with low porosity (L and D) you can clearly see the first initial step (0–200 min)

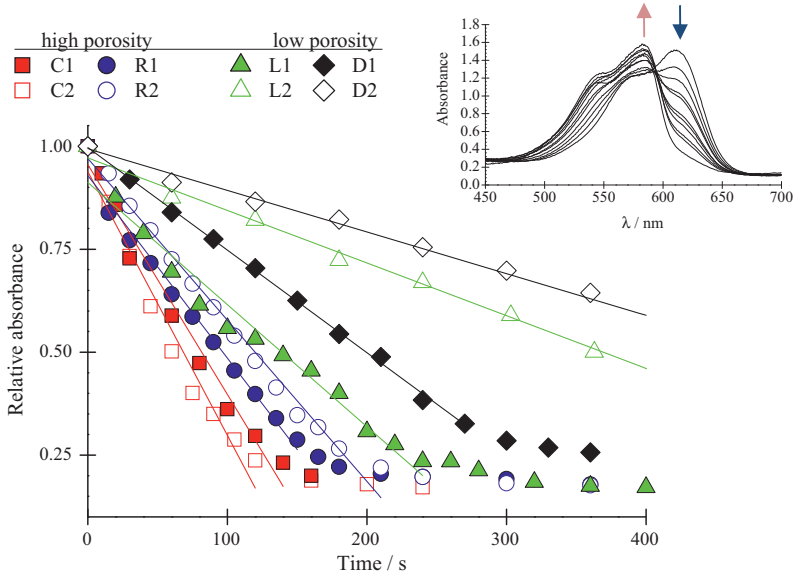

Fig. 5. Relative absorbance of Rz ink measured at 610 nm for different TiO_2/SiO_2/glass films (C1, R1, D1 and L1 having the same mass of titania) as a function of illumination time. The insert diagram is a plot of UV–vis absorption of a typical Rz ink film in contact with L1/SiO_2/glass films as a function of UVA (1.0 mW cm^{-2}) irradiation time (one spectrum every 20 s).

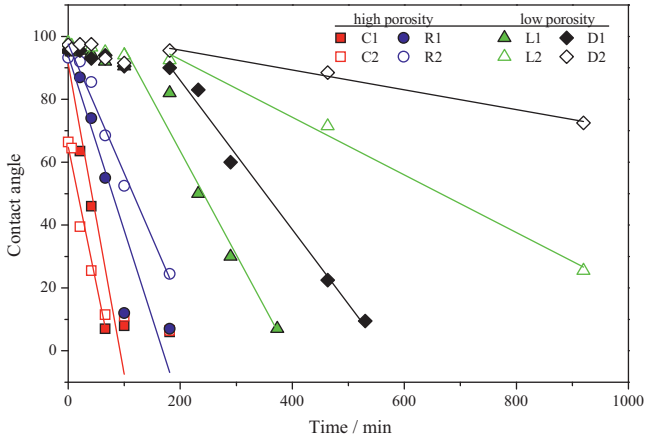

Fig. 6. MS degradation – contact angles measurement for different TiO_2/SiO_2/glass films (C1, R1, D1 and L1 same mass of titania) as a function of illumination time.

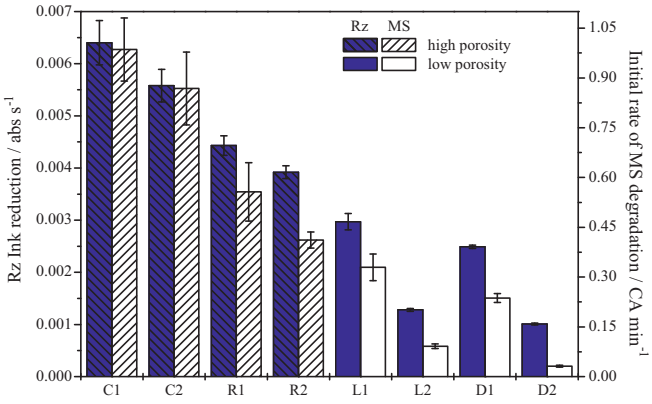

Fig. 7. Rates of Rz ink reduction and MS decomposition for TiO_2 films of various porosity and titania loading.

of degradation, where the decomposition is very slow due to the low light penetration through the MS layer. As a consequence, it is obvious, that for MS test the porosity is very important (similar like in Rz ink test).

A good correlation is noticed between the novel and the standard method. In order to quantify the data, the degradation rate of MS was obtained from the curves and the data are collected together with the Rz ink reduction in Fig. 7.

Generally, the results obtained shown the rather complex effect of the porosity of TiO_2 films on their photocatalytic performance. Especially in an aqueous media the photocatalytic activity substantially depends on the respective mechanism. The increased adsorption due to a large surface area may be beneficial when its decomposition is initiated by direct hole transfer. However, too high concentrations of adsorbed species to be degraded may even be detrimental and lead to a substantial decrease in the degradation rate [12]. AO7, which is a sodium salt of sulfonic acid, exhibits pH slightly above the isoelectric point of TiO_2. Due to this fact AO7 anion is not electrostatically attracted to the titania surface. Consequently the degradation of AO7 is mediated by primarily generated $OH^{\bullet}$. It was already observed that AO7 photocatalytic degradation led to only small change of pH. It means that the surface conditions are practically unchanged during the whole degradation and the porosity of the film does not influence the photodegradation process. Dominant role place the number of photons absorbed in the layer which is proportional to the mass of titania.

In the case of 4CP, HCl is formed during photocatalytic degradation which causes gradual decrease in pH leading to surface polarity change. However, owing to the electroneutrality of 4CP molecules, their adsorption and rate of photocatalytic degradation should not be effected. Similarly to AO7, the dominant factor is the light absorbed.

In the photocatalytic degradation of both solid and liquid layers of various substances (such as methyl stearate, stearic acid, oleic acid, and dyes) the effect of the porosity has been found mostly beneficial [5,16]. The most probable reason is the mesoporosity ensures better transport of O_2 and H_2O, which are viable for the photocatalytic degradation of deposits. This transport is often significantly hindered by a compact layer of deposited matter [17]. This general tendency is confirmed by the beneficial effect of porosity found in the degradation of relatively thick layers of Resazurin ink and methyl stearate.

4. Conclusions

It can be concluded, that for photocatalytic degradation of both model compounds (AO7 and 4CP) porosity is not important while mass of titania in layer is decisive. On the other side for MS oxidation and Rz reduction it was observed that the degradation rate increases with increasing porosity of titania layer. This means that porosity generally plays important role in photocatalytic degradations of thin organic layers.

Those results should be taken into account when the standardisation methods will be proposed, because it looks like that one single test is not enough to compare or test the photocatalytic activity of titania layers, especially when their morphological and structural properties are different.

Acknowledgements

The authors thank to Czech-Slovenian bilateral project MEB 090810. Partial financial support (project 1M0577) of the Ministry of Education, Youth and Sport of the Czech Republic and the Grant Agency of the Czech Republic (project number 104/08/0435) is also acknowledged.

References

[1] A. Fujishima., T.N. Rao, D.A. Tryk, J. Photochem. Photobiol. C: Photochem. Rev. 1 (2000) 1–21.
[2] M.I. Litter, Appl. Catal. B: Environ. 23 (1999) 89–114.
[3] S. Malato, P. Fernandez-Ibanez, M.I. Maldonado, J. Blanco, W. Gernjak, Catal. Today 147 (2009) 1–59.
[4] Y. Ao, J. Xu, D. Fu, C. Yuan, Appl. Surface Sci. 255 (2008) 3137–3140.
[5] J. Rathouský, V. Kalousek, V. Yarovyi, M. Wark, J.J. Jirkovský, J. Photochem. Photobiol. A: Chem. (2010), doi:10.1016/j.jphotochem.2010.06.002.
[6] T. Watanabe, S. Fukayama, M. Miyauchi, A. Fujishima, K. Hashimoto, J. Sol-Gel Sci. Technol. 19 (2000) 71–76.
[7] U Černigoj, U. LavrenčičŠtangar, P. Trebše, P. RebernikRibič, Acta Chim. Slov. 53 (2006) 29–35.
[8] U. Černigoj, U. LavrenčičŠtangar, P. Trebše, U. OparaKrašovec, S. Gross, Thin Solid Films 495 (2006) 327–332.
[9] J. Zita, J. Krýsa, A. Mills, J. Photochem. Photobiol. A: Chem. 203 (2009) 119–124.
[10] A. Mills, M. McGrady, J. Photochem. Photobiol. A: Chem. 193 (2008) 228–236.
[11] S.L. Murov, I. Carmichael, G.L. Hug, Handbook of Photochemistry, second ed, Marcel Dekker Inc., New York, 1993, p. 299.
[12] J. Tschirch, D. Bahnemann, M. Wark, J. Rathousky, J. Photochem. Photobiol. A: Chem. 194 (2008) 181–188.
[13] PDF-2—Powder diffraction File (ICDD—International Centre for Diffraction Data) ICDD (2005).“Powder Diffraction File,” International Centre for Diffraction Data, edited by Frank McClune, 12 Campus Boulevard, Newton Square, Pennsylvania 19073-3272.
[14] Y. Chen, E. Stathatos, D.D. Dionysiou, Surface Coat. Technol. 202 (2008) 1944–1950.
[15] M. Zlámal, J. Krýsa, J. Jirkovský, Catal. Lett. 133 (2009) 160–166.
[16] J. Rathouský, V. Kalousek, Ch. Walsh, Technical Proceedings of the 2009 Nanotechnology Conference and Trade Show, vol. 3, NSTI, Danville, USA, 2009, pp. 202–205.
[17] D. Ollis, Appl. Catal. B: Environ. 99 (2010) 478–484.